JOURNAL OF CHEMICAL INFORMATION AND MODELING

Article

pubs.acs.org/jcim

g_mmpbsa—A GROMACS Tool for High-Throughput MM-PBSA Calculations

Rashmi Kumari,[†] Rajendra Kumar,[†] Open Source Drug Discovery Consortium,[‡] and Andrew Lynn*[,†]

[†]School of Computational and Integrative Sciences, Jawaharlal Nehru University, New Delhi 110067, India

[‡]CSIR Open Source Drug Discovery Unit, Anusandhan Bhavan, Delhi 110001, India

Supporting Information

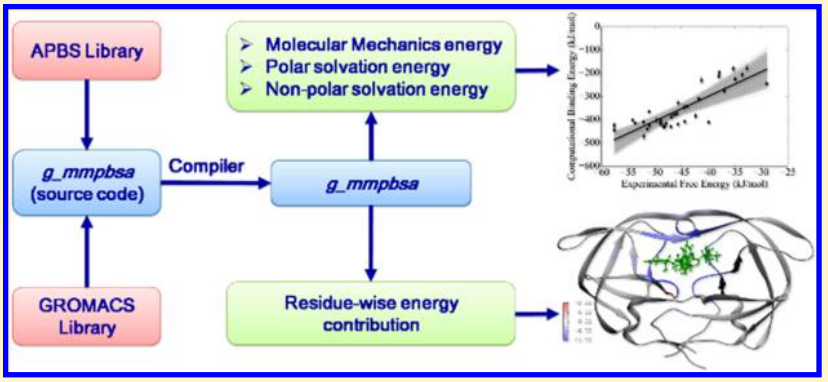

ABSTRACT: Molecular mechanics Poisson−Boltzmann surface area (MM-PBSA), a method to estimate interaction free energies, has been increasingly used in the study of biomolecular interactions. Recently, this method has also been applied as a scoring function in computational drug design. Here a new tool *g_mmpbsa*, which implements the MM-PBSA approach using subroutines written in-house or sourced from the GROMACS and APBS packages is described. *g_mmpbsa* was developed as part of the Open Source Drug Discovery (OSDD) consortium. Its aim is to integrate high-throughput molecular dynamics (MD) simulations with binding energy calculations. The tool provides options to select alternative atomic radii and different nonpolar solvation models including models based on the solvent accessible surface area (SASA), solvent accessible volume (SAV), and a model which contains both repulsive (SASA-SAV) and attractive components (described using a Weeks−Chandler−Andersen like integral method). We showcase the effectiveness of the tool by comparing the calculated interaction energy of 37 structurally diverse HIV-1 protease inhibitor complexes with their experimental binding free energies. The effect of varying several combinations of input parameters such as atomic radii, dielectric constant, grid resolution, solute−solvent dielectric boundary definition, and nonpolar models was investigated. *g_mmpbsa* can also be used to estimate the energy contribution per residue to the binding energy. It has been used to identify those residues in HIV-1 protease that are most critical for binding a range of inhibitors.

INTRODUCTION

The strength of a biomolecular interaction such as involved in recognition or catalysis can be quantified in terms of its binding free energy and a range of computational approaches can be used to estimate binding free energies. These include free energy perturbation (FEP), thermodynamic integration (TI), linear interaction energies (LIE), molecular mechanics Poisson−Boltzmann surface area (MM-PBSA), and molecular mechanics Generalized Born surface area (MM-GBSA) approaches.[1−8] Of these FEP and TI are the most rigorous but also the most computationally expensive. FEP and TI involve the transformation of a molecule from an initial to the final state over a reversible path. As a consequence, these two methods are mostly applicable to small perturbations or structural transitions.[2] FEP and TI methods are also difficult to employ in cases where large numbers of protein−ligand complexes containing structurally diverse ligands are being considered as it is necessary to generate a dual/hybrid topology for each pair.[3] An alternative is to use path independent methods such as LIE or MM-PBSA. These methods estimate the free energy using an ensemble of structures at the initial and final states making these approaches computationally highly efficient.[5,7,8]

The MM-PBSA approach has grown to be one of the most widely used methods to compute interaction energies and is often employed to study biomolecular complexes.[6] Combined with molecular dynamics (MD) simulations, MM-PBSA can also incorporate conformational fluctuations and entropic contributions to the binding energy.[6] The MM-PBSA approach combines three energetic terms to account for the change in the free energy on binding. The first term corresponds to a change

Received: January 11, 2014
Published: May 21, 2014

   dx.doi.org/10.1021/ci500020m | J. Chem. Inf. Model. 2014, 54, 1951−1962

in the potential energy in the vacuum. It includes both bonded terms such as bond, angle, and torsion energies as well as nonbonded terms such as van der Waals and electrostatic interactions. The second term accounts for the desolvation of the different species. It is quantified by the sum of two energy terms, i.e., the polar and nonpolar solvation energies using an implicit solvation model.[9−12] The third term accounts for the configurational entropy associated with complex formation in the gas phase.

The MM-PBSA method has been applied to predict binding free energies and to evaluate the relative stabilities of different biomolecular structures.[13−20] Furthermore, this method has been employed to understand biomolecular associations in detail by decomposing the total binding energy into a series of components.[7,21−24] In high-throughput docking calculations, MM-PBSA has been used to remove false positives and to discriminate between active and inactive lead molecules by rescoring configurations selected initially based on simple energetic or geometric criteria.[25−27] Recently MM-PBSA has also been combined with MD simulations to rescore a set of docked complexes significantly improving the utility of the complexes identified.[1,22,28−30] In these cases, MD simulations were used to generate an ensemble of binding conformations in the presence of explicit water, and further, the MM-PBSA approach was used to estimate the binding energy.

Despite the potential of this combined MM-PBSA and MD simulation approach, its application in high-throughput binding energy calculation is still limited. One reason for this is that while the MM-PBSA method is implemented in the AMBER package[31] the AMBER MD module, *sander/pmemd*, is not freely available, and thus, it is not easily accessible to a large community of users. MM-PBSA calculations can also be performed using other programs. For example, the simulation package GROMACS[32] can be coupled with external software such as DelPhi[33] and APBS[34] using a collection of scripts to perform MM-PBSA calculations.[35−37] However, there is no open source standalone tool that can be used to directly perform MM-PBSA calculations using GROMACS. To overcome the dependencies associated with linking DelPhi and APBS to GROMACS, we have developed an open source tool called *g_mmpbsa* in which the MM-PBSA method is implemented in the C programming language removing any runtime dependency on external software. This tool contains all the required subroutines from the GROMACS and the APBS packages to calculate the enthalpic components of the MM-PBSA interaction. In addition, *g_mmpbsa* contains routines developed in-house with improved functionality related to the handling of the trajectory files and the calculation of specific energy terms. *g_mmpbsa* also provides options to select alternative atomic radii used to determine the molecular surface during the calculation of both the polar and nonpolar solvation energy. Several alternative nonpolar solvation models along with the widely used SASA-only model are also included.[38−40] In addition, the binding energy can be decomposed on a per residue basis. *g_mmpbsa* can also be used with the NAMD[41] simulation package which, like GROMACS, is freely available.

In this paper, the functionality of *g_mmpbsa* is described in detail. The utility of *g_mmpbsa* is also demonstrated by performing MD simulations of 37 HIV-1 protease inhibitor complexes for which crystal structures are available and calculating the average binding energies from the ensemble of conformations obtained. The performance of the *g_mmpbsa* tool was assessed by calculating the Pearson correlation coefficients (r) and predictive index (PI),[42] between the predicted and the experimental binding free energies. Furthermore, the sensitivity of the results obtained to changes in the parameters used in the solvation energy calculation such as the atomic radii, solute dielectric constant, grid spacing, solute−solvent dielectric boundary definition, and the use of different nonpolar models is also presented. Finally, the energetic contributions of residues within HIV-1 protease to the total binding energy of a range of ligands are determined and compared with those from previous investigations.[21,43−45]

THEORY

In general terms, the binding free energy of the protein with ligand in solvent can be expressed as[8,9,46]

$$\Delta G_{\text{binding}} = G_{\text{complex}} - (G_{\text{protein}} + G_{\text{ligand}}) \quad (1)$$

where, G_{complex} is the total free energy of the protein−ligand complex and G_{protein} and G_{ligand} are total free energies of the isolated protein and ligand in solvent, respectively. The same equation is applicable to other types of biomolecular interactions such as protein−protein, protein−DNA complexes, etc. Furthermore, the free energy for each individual entity can be given by[7,8,14,16,47]

$$G_x = \langle E_{\text{MM}} \rangle - TS + \langle G_{\text{solvation}} \rangle \quad (2)$$

where x is the protein or ligand or protein−ligand complex. $\langle E_{\text{MM}} \rangle$ is the average molecular mechanics potential energy in a vacuum. TS refers to the entropic contribution to the free energy in a vacuum where T and S denote the temperature and entropy, respectively. The last term $\langle G_{\text{solvation}} \rangle$ is the free energy of solvation.

Molecular Mechanics Potential Energy. The vacuum potential energy, E_{MM}, includes the energy of both bonded as well as nonbonded interactions, and it is calculated based on the molecular mechanics (MM) force-field parameters.[48−50]

$$E_{\text{MM}} = E_{\text{bonded}} + E_{\text{nonbonded}} = E_{\text{bonded}} + (E_{\text{vdW}} + E_{\text{elec}}) \quad (3)$$

where E_{bonded} is bonded interactions consisting of bond, angle, dihedral and improper interactions. The nonbonded interactions ($E_{\text{nonbonded}}$) include both electrostatic (E_{elec}) and van der Waals (E_{vdW}) interactions and are modeled using a Coulomb and Lennard-Jones (LJ) potential function, respectively. Note, in the single trajectory approach, the conformation of protein and ligand in the bound and unbound forms are assumed to be identical. Thus, ΔE_{bonded} is always taken as zero.[6]

Free Energy of Solvation. The free energy of solvation is the energy required to transfer a solute from vacuum into the solvent. In the MM-PBSA approach, it is calculated using an implicit solvent model. The solvation free energy is expressed as the following two terms[9,12,51]

$$G_{\text{solvation}} = G_{\text{polar}} + G_{\text{nonpolar}} \quad (4)$$

where G_{polar} and G_{nonpolar} are the electrostatic and nonelectrostatic contributions to the solvation free energy, respectively.

Polar Solvation Energy. The electrostatic term, G_{polar}, is estimated by solving the Poisson−Boltzmann (PB) equation,[34,46,51] which is given by

$$\nabla\cdot[\varepsilon(r)\nabla\cdot\varphi(r)] - \varepsilon(r)\kappa(r)^2\sinh[\varphi(r)] + \frac{4\pi\rho^{f}(r)}{kT} = 0 \quad (5)$$

where $\phi(r)$ is electrostatic potential, $\varepsilon(r)$ is the dielectric constant, and $\rho^{f}(r)$ is the fixed charge density. The term κ^2 is related to the reciprocal of Debye length which is dependent on the ionic strength of the solution. The PB equation is a second-order nonlinear elliptic partial differential equation. For the case of $\phi\ (r) \ll kT$, $\sinh[\phi(r)] \approx \phi(r)$, the PB equation becomes linear. However, for highly charged systems, the use of the nonlinear PB equation is necessary.

Nonpolar Solvation Energy. The nonelectrostatic term of solvation free energy, $G_{nonpolar}$, includes repulsive and attractive forces between solute and solvent that are generated by cavity formation and van der Waals interactions, respectively.[38−40] It can be expressed

$$G_{nonpolar} = G_{cavity} + G_{vdW} \quad (6)$$

where G_{cavity} is work done by the solute to create a cavity in the solvent and depends on the shape and geometry of the solute. G_{vdW} is the attractive van der Waals energy between solvent and solute. These terms can be estimated using a variety of models.

SASA-Only Nonpolar Model. This is one of the most widely used nonpolar models. The solvent accessible surface area (SASA) model is based on the assumption that the SASA is linearly dependent on the $G_{nonpolar}$ term and can thus be calculated as follows:[7,11,12,14,16,46,47,52]

$$G_{nonpolar} = \gamma A + b \quad (7)$$

where γ is a coefficient related to surface tension of the solvent, A is SASA, and b is fitting parameter.

SAV-Only Nonpolar Model. According to this model, the solvent accessible volume (SAV) is assumed to be linearly proportional to the nonpolar solvation energy[39,40,53−57] and can be written as follows:

$$G_{nonpolar} = pV + b \quad (8)$$

where p is a coefficient related to pressure of the solvent, V is SAV, and b is again a fitting parameter.

SASA−SAV Nonpolar Model. In this model, the scaled particle theory (SPT)[58] approach is used to quantify the nonpolar energy using both the SASA as well as SAV.[40] This can be expressed as

$$G_{nonpolar} = \gamma A + pV \quad (9)$$

Note the models based on SASA, SAV, or their combination only account for the energy of cavity formation. The contributions due to attractive solute−solvent interactions (G_{vdW}) are not considered.

SASA−SAV−WCA Nonpolar Model. This model combines both SPT and Weeks−Chandler−Andersen (WCA) theory and takes into account cavity creation and van der Waals interactions.[39,40,58,59] The model can be expressed as

$$G_{nonpolar} = \gamma A + pV + G_{vdW} \quad (10)$$

The first two terms are the same as in eq 9 and represent the work done to form a cavity in the solvent by the solute. G_{vdW} is the attractive interaction between the solute and solvent and is modeled using the attractive term of WCA-like integral,[38,59] as described by Wagoner et al.[40] This term corresponds to the integral of the attractive term of Lennard-Jones interaction between each solute atom and the solvent outside of the cavity assuming an uniform solvent distribution.[40]

Binding Energy Decomposition. Using the *g_mmpbsa*, tool, the binding energy can be decomposed on a per residue basis. Initially the energy components E_{MM}, G_{polar}, and $G_{nonpolar}$ of individual atoms are calculated in the bound as well as the unbound form, and subsequently their contribution to the binding energy ΔR_x^{BE} of residue x is calculated as follows:

$$\Delta R_x^{BE} = \sum_{i=0}^{n} (A_i^{bound} - A_i^{free}) \quad (11)$$

where $A_i^{complex}$ and A_i^{free} are the energy of ith atom from x residue in bound and unbound forms respectively, and n is the total number of atoms in the residue. We note that energy contribution summed over all residues is equal to the binding energy, i.e. $\Delta G_{binding} = \sum_{x=0}^{m} \Delta R_x^{BE}$, where, m is total number of residues in either protein−protein or protein−ligand complexes.

METHODS

Development of *g_mmpbsa*. *g_mmpbsa* is written in the programming language C and inherits functions from GROMACS as well as APBS to calculate energy components given in eq 2, except for the entropy. Note that the PB equation solver of the APBS can be used via the iAPBS interface[60] which can be coupled to CHARMM,[61] AMBER,[62] and NAMD.[41] However, in *g_mmpbsa* APBS subroutines are called directly. This allowed us to implement alternative approaches to calculate the nonpolar solvation energy including the SAV and WCA models not available in iAPBS. The self-written as well as modified and unmodified subroutines sourced from the APBS and GROMACS package are listed in Table 1. The compiled program has no dependency on either of the two packages and can be used as a standalone tool. This tool requires four input files, namely a trajectory file (*trr* or *xtc*), a topology-parameter file (*tpr*), an index file (*ndx*), and a $G_{solvation}$ parameters file (*mdp*). Note, only the electrostatic (E_{elec}) and van der Waals (E_{vdW}) components of the vacuum potential energy (E_{MM}) have been implemented as ΔE_{bonded} is by definition zero in the single-trajectory approach.

Three alternative sets of atomic radii, namely bondi, mbondi, and mbondi2 in addition to those given within the AMBER force field are provided.[10,31,63−65] The radii values for atomtypes in case of bondi, mbondi, and mbondi2 are provided in Supporting Information Table S1. The tool also has an option to select alternative nonpolar solvation models. The solvent accessible surface area and volume was calculated using the double cubic lattice method,[66] which is implemented in *g_sas* program of GROMACS. We have slightly modified this code to calculate the SAV of individual atoms. This is necessary for the calculation of the energy contribution to the total binding energy when using the SAV-only model. As per eq 10, G_{vdW} was calculated using subroutines imported from APBS.[40]

To decompose the binding energy, at first ΔE_{MM}, ΔG_{polar}, and $\Delta G_{nonpolar}$ are separately calculated for each residue and were then summed up to obtain the contribution of each residue to the binding energy. The net energy contributions were calculated using eq 11, which considers the difference between the bound and unbound forms on a per atom basis. The $G_{nonpolar}$ energies using the SASA and SAV models were calculated using the double cubic lattice method. Contributions from the WCA model were calculated using subroutines taken

Table 1. Important Functions Imported from the GROMACS and APBS Package Including Functions Written In-House with Their Description

function name	source	description
	Reading Input Files	
read_tps_conf	GROMACS	to read tpr/tpx file
get_index	GROMACS	to read index file
ReadInput	in-house	to read parameters for solvation energy from mdp file
read_next_x	GROMACS	to read and extract each frame of trajectory in loop
	Molecular Mechanics Energy Calculation	
energy_pair	in-house	to make a list of 1−4 and nonbonded atom pairs
Vac_MM	in-house	to calculate electrostatic and van der Waals energy
	Polar Solvation Energy Calculation	
assignQR	in-house	to extract and assign charges and radius as per radius type
psize	ported from psize.py (APBS)	to calculate center of grid box as well as coarse and fine grid dimensions
makePQR	in-house	to create pqr file
apbs	APBS (modified)	to calculate polar salvation energy
	Nonpolar Solvation Energy Calculation	
SasvRad	in-house	to assign radius as per radius type
Mod_nsc_dclm_pbc	GROMACS (modified)	to calculate solvent accessible surface area and volume
apbs	APBS (modified)	to calculate WCA component of nonpolar solvation energy

from APBS. The G_{polar} term was also calculated using the subroutines imported from the APBS package.

The complete *g_mmpbsa* package includes several python scripts to perform the final statistical analysis using the energetic terms obtained and to calculate the energetic contributions of each residue in the protein−ligand or protein−protein complex. The whole package along with the source code is available for download from https://github.com/RashmiKumari/g_mmpbsa and has been tested for GROMACS versions 4.5.x/4.6.x and APBS versions 1.2.x/1.3.x. A full description of the package is available at http://rashmikumari.github.io/g_mmpbsa.

Inhibitor Data Set. To test the tool, we have compared the calculated binding energies for 37 HIV-1 protease inhibitor complexes to experimental binding energies calculated from their respective inhibition constant (K_i). These complexes have selected on the account of both a broad range of inhibition constants K_i, i.e. from 0.05 to 9600 nM (see details in Supporting Information Table S2), as well as a diverse range of structural scaffolds. The crystal structures of the complexes were downloaded from the protein data bank (www.pdb.org). The PDB IDs of these 37 HIV-1 protease complexes are as follows: 1EC2, 1D4H, 1EBZ, 2AQU, 1EBW, 1EC3, 1EC1, 1T7K, 1D4I, 2CEJ, 1EC0, 2UXZ, 1W5Y, 1W5X, 1D4J, 2CEN, 1W5V, 1G35, 2BQV, 1G2K, 2CEM, 1AJX, 1AJV, 1IZH, 2PSU, 1XL5, 2PSV, 2QNN, 2UY0, 2PWR, 2PWC, 2QNP, 2QNQ, 3BGB, 1XL2, 2PQZ, and 3BGC.

Molecular Dynamics Simulations. Each of the 37 HIV-1 protease inhibitor complexes has been simulated for a period of 10 ns in explicit water. To prepare the starting structure for each simulation, the ligand coordinates were extracted from the PDB structure file of the complex. Where required, hydrogen atoms were added using the Open-Babel package.[67] Partial atomic charges were then assigned based on the AM1-BCC method[68,69] using the *antechamber* program of AmberTools.[62] The van der Waals and bonded parameters for the ligand were taken from the general amber force field (GAFF).[50] The full Amber topology/coordinate files were created using the programs *parmchk* and *tleap* of the AmberTools package.[62] The AMBER format files of ligands were converted to the GROMACS format using the *acpype* python script.[70]

During the preparation of the protein structure for simulation, the protonation state of ASP25 in both chains of HIV-1 protease was determined for each complex in the presence of ligand using the PROPKA server.[71] The protonation state obtained was used during the MD simulations. The specific protonation state of ASP25 in each complex is listed in the fourth column of the Supporting Information Table S2. Note that, in the case of all complexes, one of the two ASP25 residues was charged. The topology and coordinate files for the protein were generated using *pdb 2gmx* program of the GROMACS package taking parameters from the AMBER99SB force field.[48] The coordinate and topology files of the protein and the ligands were then merged to obtain the final starting structure and topology file for each complex.

MD simulations were performed using GROMACS-4.5.5.[32] The complex was placed in the center of a dodecahedron periodic box and solvated by the addition of TIP3P water molecules.[72] The net charge on the system was then neutralized by adding counterions as required. The ionic strength was adjusted by the addition of 0.150 M of NaCl. The energy was minimized using the steepest descent algorithm. The system was then heated to 300 K during a 200 ps constant volume simulation with 1 fs time step. The pressure was then equilibrated to 1 atm during a 500 ps NPT simulation with 2 fs time step. In both simulations, all heavy atoms were position restrained with the force constant of 1000 kJ/(mol nm^2). The position restraint was gradually removed during a 1 ns simulation with a time step of 2 fs. Both temperature and pressure were regulated using the Berendsen algorithm.[73] Production simulations were performed for 10 ns with a 2 fs time step. The temperature and pressure were maintained at 300 K and 1 atm using the v-rescale temperature[74] and Parrinello−Rahman[75] pressure coupling method. The time constant for the temperature and pressure coupling was kept at 0.1 and 1 ps, respectively. The short-range nonbonded interactions were computed for the atom pairs within the cutoff of 1 nm, while the long-range electrostatic interactions were calculated using particle-mesh-Ewald summation method with fourth-order cubic interpolation and 1.2 Å grid spacing.[76] All bonds were constrained using the parallel LINCS method.[77,78]

Calculation of Binding Energy. The binding energy was calculated using *g_mmpbsa*, and the results obtained were compared with experimental binding free energy derived from the inhibition constant (K_i). The inhibition constant of the reversible competitive inhibitors are equivalent to the dissociation constant (K_d).[79] Therefore, the binding free energy was calculated using the following equation:

$$\Delta G_{expt} = -RT \ln(1/K_i)$$

where R and T are the gas constant and the temperature.

The energy components E_{MM}, G_{polar}, and $G_{nonpolar}$ of each complex were calculated for 17 snapshots extracted every 0.5 ns from the production trajectories from 2 to 10 ns. E_{MM} was calculated using the LJ and Coulomb potential. To calculate

Table 2. Parameter Values Used in $G_{nonpolar}$ Models during Binding Energy Calculations for Testing of Tool

model type	SASA[a]	SAV[b]	SASA−SAV[b]	SASA−SAV−WCA[b]	SASA−WCA[c]	SAV−WCA[c]
probe radius, ρ (Å)	1.4	1.29	1.25	1.25	ρ_{SASA} = 0.31	ρ_{SAV} = 1.37
					ρ_{WCA} = 0.406	ρ_{WCA} = 0.406
γ (kJ mol^{-1} Å^{-2})	0.022 67		−0.029 28	0	0.393 71	
p (kJ mol^{-1} Å^{-3})		0.234 304	0.217 56	0.230 12		0.161 92
offset, b (kJ mol^{-1})	3.849 28	0			−4.296 13	3.277 74
bulk water density, bconc (Å^{-3})				0.033 428	0.033 33	0.033 33
grid spacing (Å)				0.4, 0.4, 0.4	0.4, 0.4, 0.4	0.4,0.4, 0.4
sdens				200	200	200
dpos (Å)				0.05	0.05	0.05

[a]Values from ref 16 by Wang et al. [b]Values from ref 40 by Wagoner et al. [c]Values from ref 39 by Tan et al.

G_{polar}, a box was generated using the extreme coordinates of the molecular complex in each dimension. The box was then expanded in each dimension by 2-fold to obtain a coarse-grid box (cfac = 2). A finer grid-box is then placed within the coarse grid-box extending 20 Å (fadd = 20) from the complex's extreme coordinates in each direction. An ionic strength of 0.150 M NaCl with radii of 0.95 and 1.81 Å for sodium and chloride ions respectively was used during all G_{polar} calculations. The values for the vacuum (vdie) and solvent (sdie) dielectric constants were taken as 1 and 80 respectively. The solute (pdie) dielectric constant was assigned a value of two or eight in order to study the sensitivity of the energy to changes in this parameter. The linear and nonlinear PB equation was solved using APBS. $G_{nonpolar}$ was calculated using different nonpolar models using the parameters provided in Table 2. Subsequently, the binding energy of each snapshot was calculated for each complex using a combination of eqs 1 and 2. Note that the entropy contribution was not included in the binding energy.

To calculate the average binding energy and the associated confidence intervals, a bootstrap analysis was performed. This bootstrap analysis requires that the energy values of the snapshots are uncorrelated. To demonstrate that the values are not correlated, the autocorrelation function of binding energies values of snapshots extracted at every 0.01 ns from the trajectory 2−10 ns for each complex was calculated (see details in Supporting Information Table S3). A maximum autocorrelation time of ∼0.45 ns was obtained. Thus, the snapshots extracted every 0.5 ns were assumed to be uncorrelated. The confidence intervals were estimated using 5000 bootstrap runs on the 17 binding energies values for each protein−ligand complex. The averages of the binding energies obtained from the bootstrap analysis together with their respective confidence intervals are provided as Supporting Information (Figures S2−4, S7, and S9A−B). This bootstrap procedure, which uses snapshots extracted at 0.5 ns, was used to study the sensitivity of predicted binding energies to the input parameters that were used for calculating the solvation energy.

Bootstrap Analysis of the Correlation. Because of the structural diversity in the ligands considered, the fluctuations in binding energy values were expected to be large (5−15 kJ/mol).[19,80] This in turn would result in a large uncertainty in the correlation coefficients obtained. Therefore, 99% confidence intervals for correlation coefficients were calculated also using a bootstrap approach. This was implemented in two steps to maximize the uncertainty in correlation. In the first step, the binding energies for each complex obtained from the 5000 bootstrap runs as described above were sorted in increasing order. Twenty-one energy values were chosen at equal intervals from the sorted list for each complex. Then, a second bootstrap analysis was performed to calculate the distribution of the correlation coefficients. During this analysis, sample complexes were chosen at random from the 37 complexes available. Then an average binding energy was chosen randomly from the list of 21 average binding energies for the respective complexes. A correlation coefficient was then calculated with respect to the experimental binding free energies. The convergence in the confidence interval of the binding energies was then evaluated. It was observed that 1000 steps were sufficient for the standard error in the energy values to converge. However, at least 5000 steps were required to reach a stable distribution of the correlation coefficients. A flowchart depicting this two step bootstrap analysis procedure is also provided as Supporting Information (Figure S1).

RESULTS AND DISCUSSION

g_mmpbsa. *g_mmpbsa* was developed to enable the use of the MM-PBSA method in conjunction with the GROMACS package. The *g_mmpbsa* interface is similar to other GROMACS tools and is aimed at existing GROMACS users. An overview of the implemented scheme to calculate the three energetic terms E_{MM}, G_{polar}, and $G_{nonpolar}$ is illustrated in Figure 1. The input parameters for the calculation of G_{polar} are the same as those used in APBS, which are listed in the online documentation for *g_mmpbsa*. APBS solves the PB equation (eq 5) using a finite difference multigrid focusing method.[34] The input parameters for $G_{nonpolar}$ may vary in accordance with the choice of the nonpolar model (eq 7−10). *g_mmpbsa* provides the flexibility to change and refine the input parameters for the calculation of the solvation energy as required. Furthermore, to improve computational efficiency, *g_mmpbsa* makes use of the parallel threading routines implemented in the APBS package.

For reasons of computational efficiency and because MM-PBSA poorly predicts the binding energy associated with large conformational transitions;[6,81] the single trajectory approach in which it is assumed the conformational space accessible to the two binding species is unchanged on binding, has been implemented. Using the single trajectory approach only the nonbonded energetic terms E_{elec} and E_{vdW} needs to be calculated because the bonded terms get canceled. Nevertheless, one could use the tool in conjunction with the multiple trajectory (i.e., allowing the conformations to vary) approach if required, as E_{MM} for an individual molecule can be calculated using the *mdrun* module of the GROMACS package.

The current implementation of the MM-PBSA method within *g_mmpbsa* does not include the calculation of entropic terms and therefore in principle is unable to give the absolute

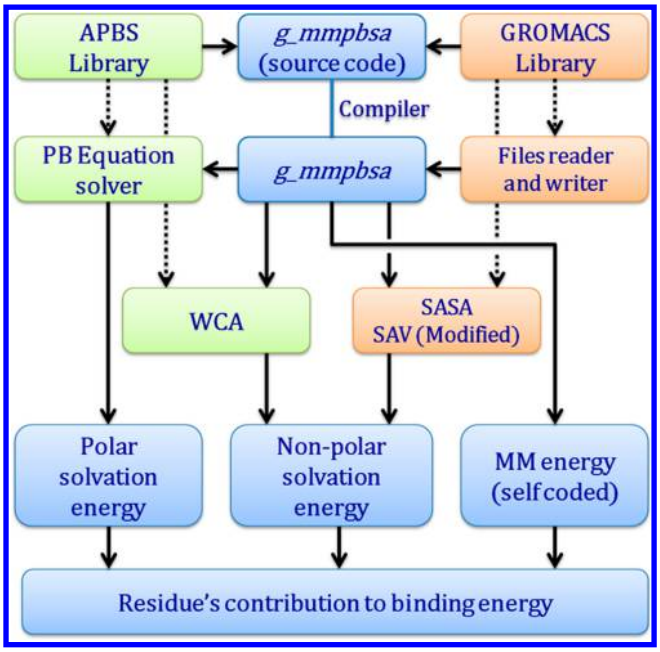

Figure 1. Schematic representation of the MM-PBSA method implemented in the *g_mmpbsa* tool.

binding energy.[8] The tool is thus suited for calculating relative binding energies, for example to compare different ligands binding to the same receptor protein. The calculation of the entropic contribution to the binding free energy is a challenging problem. Several methods have been proposed that can be used to estimate the entropy of a molecule.[82−89] However, all of these approaches are time-consuming, and the magnitude of standard error is high compared to the other energetic terms.[6,29,37] In addition, the net entropic contribution is often small, and multiple studies have suggested that including corrections for changes in the configurational free energy of the system lead to only a small improvement in the correlation with experiment.[15,18,29] If required, one can calculate the entropic contribution using modules available with the GROMACS package.

Note, wrapper scripts such as GMXAPBS can also be used to perform MM-PBSA calculations in conjunction with the GROMACS package.[34−37] The advantage of *g_mmpbsa* over such scripts is that the energetic components can be calculated in a single step without the need to parse the output files from multiple programs. Additionally, by integrating the routines directly at the source-code level, the compiled program is computationally efficient in performing only those calculations directly related to the MM-PBSA approach. *g_mmpbsa* also provides options to use alternative atomic radii together with three alternative nonpolar models, i.e., SASA, SAV, and WCA. Although subroutine to calculate SAV is imported from GROMACS module *g_sas*, its decomposition at the atomic level has not previously been implemented in either the GROMACS or the APBS package. In addition, the decomposition of the interaction energy on a per atom basis has been implemented.

Comparison with AMBER MM-PBSA. To compare the accuracy of *g_mmpbsa* with the widely used AMBER MM-PBSA package,[31] three HIV-1 protease inhibitor complexes were considered (S1−1, S1−2, and S1−3)[90] for which binding energies calculated using *mm_pbsa.pl* were available.[90] The binding energy components of these three inhibitors were recalculated using the *g_mmpbsa* for the MD trajectories provided by the authors (Table 3). Snapshots extracted every 0.01 ns were used for the calculation, to be consistent with the previous study. Input parameters for E_{MM} and $G_{nonpolar}$ were also the same as the previous study.[90] To solve the PB equation, *g_mmpbsa* uses the APBS package whereas *mm_pbsa.pl* uses the PBSA program of the AMBER suite.[31] A list of the input parameters used for G_{polar} calculation in the two packages is given as Supporting Information Table S4.

As seen in Table 3, the energies obtained using *g_mmpbsa* and the AMBER MM-PBSA package is similar, in general within 1−2 kcal/mol except for G_{polar}. The differences in G_{polar} values are likely to be caused by differences between the different algorithms, implemented in APBS and PBSA. Note although the differences are well within the standard deviations, in principle one should obtain identical value. The discrepancy most likely reflect minor differences in the implementation of the AMBER force field used in AMBER and GROMACS and differences in the precision in which the coordinates are stored.

Testing of Implementation. To test the performance of *g_mmpbsa*, average binding energies of 37 HIV-1 protease inhibitors were calculated, and the Pearson correlation coefficient (r) between the predicted and the experimental binding free energy computed. Additionally, we calculated the predictive index (PI), which quantifies the quality of the prediction of the relative binding energies. As discussed earlier, the solvation energy is dependent on a number of input parameters. Therefore, we studied the sensitivity of the *g_mmpbsa* results obtained to changes in values of the atomic radii, solute dielectric constant, grid spacing, and the solute surface definition.[10,29,91−93]

Impact of Changing the Dielectric Constant, Atomic Radii, and Grid Resolution. Most previous studies use a uniform value for the solute dielectric constant, ε_{solute} during the calculation of G_{polar} despite there being a nonuniform charge distribution within the solute.[46,51,94] Furthermore, the molecular surface, which serves as a dielectric and the ionic boundary in the implicit solvent model, is determined based on a given set of atomic radii.[33,38,43,94] Thus, the interaction energy

Table 3. Comparison of Binding Energy Components Obtained from AMBER MM-PBSA and *g_mmpbsa*[a]

	program	ΔE_{elec}	ΔE_{vdW}	ΔG_{polar}	$\Delta G_{nonpolar}$	$\Delta G_{binding}$
S1−1	*mm_pbsa.pl*	−53.9 ± 5.0	−73.5 ± 3.6	106.0 ± 9.2	−9.9 ± 0.2	−31.3 ± 7.5
	g_mmpbsa	−54.2 ± 5.1	−72.7 ± 3.6	102.9 ± 6.9	−9.6 ± 0.4	−33.7 ± 6.8
S1−2	*mm_pbsa.pl*	−45.4 ± 4.7	−84.6 ± 4.0	99.7 ± 7.9	−10.1 ± 0.2	−40.5 ± 6.6
	g_mmpbsa	−46.0 ± 3.9	−82.2 ± 3.6	94.5 ± 4.4	−10.2 ± 0.4	−43.9 ± 4.6
S1−3	*mm_pbsa.pl*	−61.7 ± 8.1	−62.6 ± 4.0	112.9 ± 11.8	−8.5 ± 0.3	−19.9 ± 15.0
	g_mmpbsa	−62.5 ± 5.2	−61.0 ± 2.8	117.4 ± 6.3	−8.5 ± 0.4	−14.6 ± 6.1

[a]The energies are in kilocalories per mole.

can be highly dependent on the precise choice of the radii used in the calculation. Therefore, both the choice of ϵ_{solute}, as well as the atomic radii, may affect G_{polar} and thus the correlation between the predicted and experimental binding energies.[10,29,91,92] The other aspect which can affect the calculation of G_{polar} is the precision with which the PB equation is solved which is primarily determined by the grid spacing.[46,95]

In a previous study, Yang et al.[29] showed based on multiple data sets that the correlation between the calculated and experimental binding energies improved over the range ϵ_{solute} = 2−4 and effectively plateau between ϵ_{solute} = 4 and 8. To investigate the influence of varying the dielectric constant, atomic radii, and the grid resolution, the binding energies have been calculated using four sets of atomic radii, i.e., amber, bondi, mbondi, and mbondi2 and two values of ϵ_{solute}, i.e., 2 and 8. In these calculations, G_{polar} was calculated by solving both the linear (LBPE) and nonlinear (NPBE) PB equation using grid resolutions of 0.5 and 0.2 Å. The $G_{nonpolar}$ term was calculated using the SASA model (eq 7 and Table 2). Comparisons of the computed energies with the experimental binding energies are given as Supporting Information (Figures S2−4). The deviations between the computed and experimental energies were quantified by the mean absolute deviation (MAD) and are also provided as Supporting Information (Figures S5I−L and S6). The MAD values vary approximately from 50−180 kJ/mol depending on the input parameters used for the calculation of the binding energies. The smallest MAD value (∼50 kJ/mol) was observed for the amber radii set using NPBE, ϵ_{solute} = 2 and 0.5 Å grid resolution. Clearly, the binding energy calculation is highly sensitive to the input parameters. Furthermore, the binding energies are in general overestimated by 2−5 times depending on the combination of parameters used. Note, MAD quantifies the absolute deviation between the predicted and experimental energies. However, in the present work, the ability of the model to predict relative differences between the binding energies is more relevant.

To determine the predictive ability of the model, distributions of the correlation coefficient between the predicted and experimental binding energies as well as the associated PI together with their confidence intervals were calculated. The correlation distributions were found to be similar irrespective of the set of radii used, whether ϵ_{solute} was 2 or 8, whether grid resolution was 0.5 or 0.2 Å and whether LBPE or NPBE was used. This is illustrated in Figures 2A and B which shows the results for solving NPBE at 0.2 Å grid resolution using ϵ_{solute} = 2 and 8, respectively. The PI distributions are also comparable to each other (Figure 2C−D). The distributions of the correlation and PI for the other combinations of input parameters are provided as Supporting Information (Fig S5A−H). Using the parameters NBPE, ϵ_{solute} = 8, and 0.2 Å grid resolution, the average correlation and PI values (i.e., 0.8 and 0.75) for each of the four sets of radii were identical (Figures 2B and D). The improvement in the average correlation obtained using ϵ_{solute} = 2 or 8 was less significant for each set of radii used. Further, the bondi radii showed the smallest uncertainty irrespective of the different combination of parameter used. In addition, when using this set of radii the results were less sensitive to changes in the values of ϵ_{solute}, grid resolution and the PB equation used. Therefore, all further calculations in the present work are performed using the bondi radii and ϵ_{solute} = 2 by assuming that the use of ϵ_{solute} = 8 will yield a similar result.

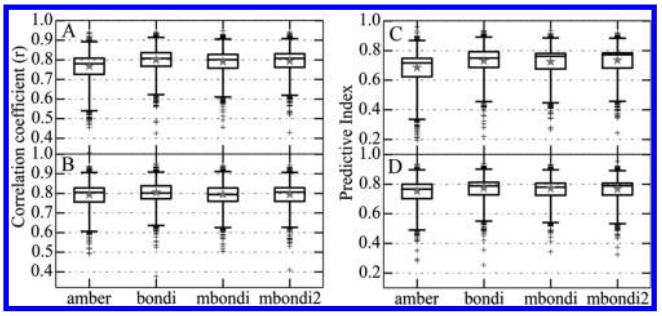

Figure 2. Influence of dielectric constant with grid resolution 0.2 Å and NPBE solver on correlation. Box shows 50% region of the obtained correlation distribution from boot-strapping. Horizontal line shown inside box depicts mode of the distribution. Error bar shows 99% region of the distribution. Symbols (+) outside the error bar show the remaining 1% of the distribution. The average correlation coefficient is shown by an asterisk. The obtained correlation distributions are shown for (A) ϵ_{solute} = 2, (B) ϵ_{solute} = 8. The predictive index obtained for the same parameters are also shown for (C) ϵ_{solute} = 2, (D) ϵ_{solute} = 8.

Impact of Using Different Nonpolar Solvation Models for Binding Energy Calculation. In several recent investigations, nonpolar solvation energy obtained using the widely used SASA-only model correlates poorly with those obtained from the explicit solvation simulations.[38−40] Several other models (eqs 8−10) have, however, been developed which achieve a better agreement.[38−40] The parameters for these models' have been optimized based on explicit solvent simulations and validated against solvation free energies. *g_mmpbsa* provides options to use three alternate nonpolar models. The influence of the choice of model on the binding energy was therefore examined. $G_{nonpolar}$ values were calculated using these different nonpolar models with the parameters provided in Table 2. The remaining two energy components, G_{polar} and E_{MM} values were obtained using bondi radii and ϵ_{solute} = 2. The final binding energies were calculated and compared with experimental binding energies and are provided as Supporting Information (Figure S7). To compare the quality of predictions with respect to the required computational time, we considered G_{polar} calculated using both 0.5 and 0.2 Å grid resolutions with LPBE and NPBE, respectively.

The correlation calculated between experimental and predicted binding energy is shown in Figure 3. As seen in

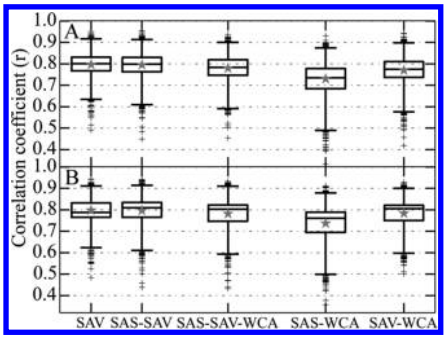

Figure 3. Influence of nonpolar models on the correlation coefficient. Box, horizontal line inside box, error bar, (+) symbols and asterisks represent similar information as described in Figure 2. The following are the parameters values/choices taken for the G_{polar}. (A) LPBE, ϵ_{solute} = 2, and 0.5 Å grid resolution. (B) NPBE, ϵ_{solute} = 2, and 0.2 Å grid resolution.

dx.doi.org/10.1021/ci500020m | J. Chem. Inf. Model. 2014, 54, 1951−1962

Figure 3, the correlation distributions obtained with SAV, SAS−SAV, SAS−SAV−WCA, and SAV−WCA models are comparable irrespective of the grid resolution and PB equations that were used in the G_{polar} calculation. These distributions are also similar to that of the widely used SASA-only model (see in Figure 2A and Supporting Information Figure S5A for bondi radii set). However, correlation distributions of the SAS-WCA model showed lower values compared to that of the SASA-only model. The PI distributions were also comparable to each other for nonpolar models SAV, SAS−SAV, and SAS−SAV−WCA (see details in Supporting Information Figures S8A−B). However, PI distributions of both SAV−WCA and SAS−WCA models showed lower values compared to that of the SASA-only model.

These results suggest that the inclusion of the SAV and WCA models do not improve the prediction of the relative binding energy when compared to the widely used SASA-only model. The parameters of these models require further optimization to improve the prediction of the binding energy of macromolecular complexes. Overall, the correlations obtained were similar to the use of SASA-only, SAV-only, and SASA−SAV models for the current data set. Additionally, the SAV-only and SASA−SAV model overestimate the binding energy by about 8−10-fold, and are therefore not suitable to predict the accurate binding energy of a specific inhibitor. Note that the value of $G_{nonpolar}$ calculated using different models were independent of the grid resolutions.

Impact of Solute Surface Definition on the Correlation. Apart from the atomic radius, dielectric constant and, grid resolution, molecular surface definition may affect the polar-solvation energy. As discussed in the earlier sections, the solute surface determines the dielectric and ionic boundary, and definition of these boundaries are likely to affect the accuracy of polar solvation energy calculated by finite difference PB method.[93,95] In all the above-discussed energy calculations, we used solvent excluded surface (SES) to define the dielectric and ionic boundary[96,97] for the G_{polar} calculation, which was further smoothed by a nine point harmonic averaging method to reduce the sensitivity caused by the discrete grid points.[98] Alternatively, these boundaries can also be defined by the vdW surface of the solute, which was smoothed using a simple polynomial function.[99,100]

We studied the impact of this particular boundary definition on the binding energy and its correlation with the experimental free energy. At first, we calculated the polar solvation energy by considering the vdW surface definition (input keyword: srfm = spl4) while keeping all other parameters the same as listed for Supporting Information Figure S5A and using bondi radii. The E_{MM} values were obtained using $\epsilon_{solute} = 2$. $G_{nonpolar}$ values were calculated using SASA-only and SAV-only model. The final binding energies were calculated and compared with the experimental binding energies and are provided as Supporting Information (Figure S9A−B). Further, the correlation with the experimental binding energies were calculated and illustrated in Figure 4. For both the SASA-only and the SAV-only nonpolar model, the average correlations and their confidence interval were improved to 0.85 and 0.7−0.95, respectively in comparison to all of the above obtained correlations. Similarly, the average PI and their confidence interval also improved to 0.8 and 0.6−0.9, respectively (see details in Supporting Information Figure S9C). The binding energies were overestimated with both the models; however with the SASA-only model showing larger value than the SAV-only model (see details in Supporting Information Figure S9D).

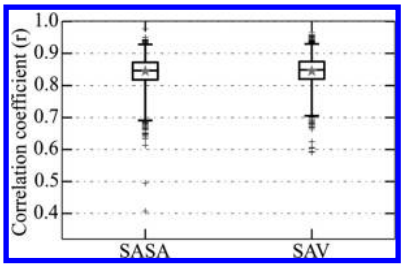

Figure 4. Influence of the surface definition parameter of polar salvation energy on the correlation using SASA-only and SAV-only model. Box, horizontal line inside box, error bar, (+) symbols and asterisks represent similar information as described in Figure 2. The surface is defined as vdW surface of the solute and is smoothed using the seventh-order polynomial function with smoothening window of 0.3 Å. The polar solvation energy was calculated using LPBE on the grid point spaced by 0.5 Å and $\epsilon_{solute} = 2$.

The smoothed vdW surface used during the G_{polar} calculation resulted in the maximum correlation between the computed and experimental binding energy for the current data set. However, binding energies were overestimated by using this surface, and therefore, it is not suitable for the absolute binding energy prediction of a particular complex. Since the binding energy appears to be sensitive to the surface definitions, the optimal choice for these parameters will depend on the details of the molecular system.

Binding Energy Decomposition. To understand protein−ligand association at molecular level, it is sometimes helpful to determine the protein residues that interact with the ligand. The *g_mmpbsa* tool decomposes total binding energy into the contribution made by each residue enabling a comparison of the relative contribution of residues to the overall binding energy. To test this implementation, we calculated per residue energy contributions for the 20 most potent HIV-1 protease inhibitor complexes (Figure 5A). As can be seen, the energy contribution profiles are similar for all the complexes. The residues strongly interacting with ligands are ARG8, the catalytic region (residues 25 to 30), the flap region (residues 47 to 50), and the C-terminal region (residues 80 to 85) (Figure 5A and B). This result is in good agreement with the energy calculated by MM-GBSA methods in the previous studies.[21,43−45] Note, the binding energy is decomposed simultaneously during its calculation without additional computational expense.

Application of *g_mmpbsa* in High-Throughput Binding Energy Calculation. As extensively discussed in a recent review by Homeyer et al., MM-PBSA has many limitations.[6] In particular, it often overestimates the binding free energy.[18,29,80,81,101] Despite these limitations Homeyer et al. argues that, the method has potential to be used in prediction of relative binding energy, to rescore docked complexes, and to study molecular recognition process in the biomolecular complexes.[6] The binding energy calculated using the *g_mmpbsa* showed an apparent correlation of 0.80−0.85 with the experimental binding free energy. One reason *g_mmpbsa* was developed was to enable the MM-PBSA approach to be tested in high-throughput binding energy calculations in conjugation with the high-throughput MD simulations.

We monitored both simulation and binding energy calculation time to get an estimate of the computational time

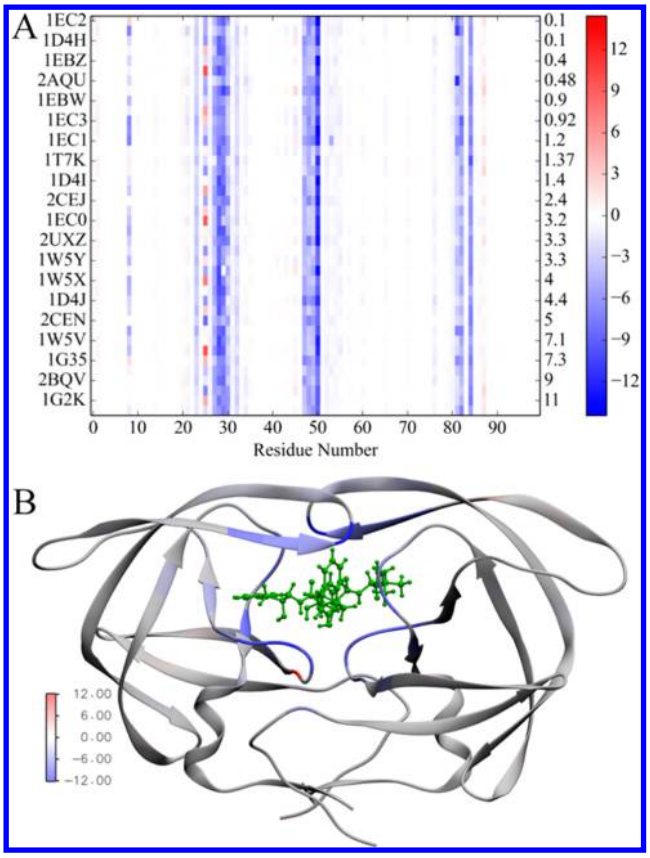

Figure 5. Energetic contribution of HIV-1 protease residues in the binding. Energies are given as kilojoules per mole. The residuewise energy contribution was calculated using free energy decomposition scheme of the tool *g_mmpbsa*. (A) The binding energy contributions of residues shown for both chain of 20 potent HIV-1 protease inhibitors. The inhibitors are given by the PDB ID of the respective complex. (B) The mapping of energy contribution on the structure of a HIV-1 protease inhibitor complex (PDB ID: 1EBZ) is made using *energy2bfac*.

on a desktop computer with Intel i5-2500, 3.3 GHz quad-core processor, and 8 GB RAM. A maximum simulation rate of ∼8 ns per day was observed for ∼30 000 atoms with the MD input parameters that are discussed in the Methods section. By solving the LPBE on 0.5 Å grid resolution (cfac = 2 and fadd = 20), the binding energy was calculated with an approximate rate of one configuration per minute. Additionally, the binding energy calculation time could be reduced significantly by using fewer snapshots extracted at larger time-difference and using bootstrap analysis to get the average binding energies (see details in Supporting Information Table S3). Note that the autocorrelation time is sensitive to the considered molecular system; consequently, the time-difference of the extracted snapshots should be considered carefully for the bootstrap analysis. These above observations suggest that *g_mmpbsa* could be used for high-throughput binding energy calculations on suitable molecular systems.

CONCLUSIONS

MM-PBSA is widely used to calculate the binding energy of biomolecular complexes and its conjugation with the MD simulations is an efficient method to study biomolecular association. It can also be used to rescore a set of docked complexes improving the ability to distinguish between active and inactive lead molecules.[25,27,102] Although implemented in the AMBER package, no open source standalone tool is available that can be used to directly perform MM-PBSA calculations using packages such as GROMACS. To overcome this limitation, we have developed an open source tool *g_mmpbsa*. The tool is written in C using subroutines from the GROMACS and APBS packages. It is a standalone tool and can be used to calculate binding energies of biomolecular complexes from the MD trajectories. The *g_mmpbsa* user interface is similar to other GROMACS modules and can be easily used by existing GROMACS users. *g_mmpba* has the option to select different types of atomic radii for the calculation of the polar solvation energy. The tool also provides a choice of nonpolar solvation models. Finally, *g_mmpbsa* can be used to decompose the total calculated binding energy into contributions per residue.

The tool is tested by comparing the calculated relative binding energy with the experimental binding free energies of 37 structurally diverse HIV-1 protease inhibitor complexes for several combinations of input parameters and nonpolar solvation models. For the current data set, a maximum average correlation (0.85) and PI (0.8) with smallest uncertainty was obtained with the polar solvation input parameters of bondi radii set, 0.5 Å grid resolution, ϵ_{solute} = 2, LPBE solver, and smoothed vdW surface, along with both the SASA-only and SAV-only models. Overall the results obtained using *g_mmpbsa* were comparable to results obtained previously with the AMBER package. Given the enhanced functionality and the computational efficiency of *g_mmpbsa* compared to existing approaches, we feel this tool will facilitate the use of the MM-PBSA method in a wide range of applications.

ASSOCIATED CONTENT

Supporting Information

Table S1 contains sets of the atomic radii implemented in g_mmpbsa tool. Table S2 provides detailed information of the data set studied. Table S3 compares the binding energies obtained using 800 and 17 snapshots with direct and boot-strap analysis method respectively. Table S4 lists the input parameters used to calculate polar solvation energy using *g_mmpbsa* and *mmpbsa.pl*. Figure S1 describes the schematic procedure to calculate correlation coefficient and confidence interval using bootstrap analysis. Figures S2-S9 show the comparison of experimental binding energies with predicted binding energies calculated using different combinations of input parameters. This material is available free of charge via the Internet at http://pubs.acs.org.

AUTHOR INFORMATION

Corresponding Author

*E-mail: andrew@jnu.ac.in.

Author Contributions

Rashmi Kumari has developed the tool and tested the tool performance under the guidance of Andrew Lynn. Rajendra Kumar has contributed to code writing and debugging and editing of the manuscript.

Notes

The authors declare no competing financial interest.

ACKNOWLEDGMENTS

We would like to acknowledge financial support from the Open Source Drug Discovery (OSDD) in part. Rashmi Kumari is

supported by Council of Scientific and Industrial Research (India) as Senior Research Fellowship. We sincerely thank Prof. Alan E. Mark for extensively reading and correcting the manuscript. The authors thank Prof. G. N. Sastry for providing the MD trajectories that were used to compare the tool performance with AMBER MM-PBSA package.

■ ABBREVIATIONS

MD, molecular dynamics; MM-PBSA, molecular mechanics Poisson−Boltzmann surface area; OSDD, Open Source Drug Discovery; MM, molecular mechanics; PB, Poisson−Boltzmann; LPBE, linear Poisson−Boltzmann equation; NPBE, nonlinear Poisson−Boltzmann equation; vdW, van der Waals; SES, solvent excluded surface; SAS, solvent accessible surface; SASA, solvent accessible surface area; SAV, solvent accessible volume; SPT, scaled particle theory; GAFF, general amber force field; WCA, Weeks−Chandler−Andersen; LJ, Lennard-Jones; corr-50, 50% region of correlation coefficient distribution; corr-99, 99% region of correlation coefficient distribution

■ REFERENCES

(1) Parenti, M. D.; Rastelli, G. Advances and applications of binding affinity prediction methods in drug discovery. *Biotechnol. Adv.* **2012**, *30*, 244−250.
(2) Meirovitch, H. Recent developments in methodologies for calculating the entropy and free energy of biological systems by computer simulation. *Curr. Opin. Struct. Biol.* **2007**, *17*, 181−186.
(3) Kollman, P. Free energy calculations: Applications to chemical and biochemical phenomena. *Chem. Rev.* **1993**, *93*, 2395−2417.
(4) Ytreberg, F. M.; Swendsen, R. H.; Zuckerman, D. M. Comparison of free energy methods for molecular systems. *J. Chem. Phys.* **2006**, *125*, 184114.
(5) Foloppe, N.; Hubbard, R. Towards predictive ligand design with free-energy based computational methods? *Curr. Med. Chem.* **2006**, *13*, 3583−3608.
(6) Homeyer, N.; Gohlke, H. Free Energy Calculations by the Molecular Mechanics Poisson−Boltzmann Surface Area Method. *Mol. Inform.* **2012**, *31*, 114−122.
(7) Gohlke, H.; Kiel, C.; Case, D. A. Insights into protein-protein binding by binding free energy calculation and free energy decomposition for the Ras-Raf and Ras-RalGDS complexes. *J. Mol. Biol.* **2003**, *330*, 891−913.
(8) Kollman, P. A.; Massova, I.; Reyes, C.; Kuhn, B.; Huo, S.; Chong, L.; Lee, M.; Lee, T.; Duan, Y.; Wang, W.; Donini, O.; Cieplak, P.; Srinivasan, J.; Case, D. A.; Cheatham, T. E., 3rd Calculating structures and free energies of complex molecules: combining molecular mechanics and continuum models. *Acc. Chem. Res.* **2000**, *33*, 889−897.
(9) Gilson, M. K.; Honig, B. Calculation of the total electrostatic energy of a macromolecular system: solvation energies, binding energies, and conformational analysis. *Proteins* **1988**, *4*, 7−18.
(10) Rizzo, R. C.; Aynechi, T.; Case, D. A.; Kuntz, I. D. Estimation of absolute free energies of hydration using continuum methods: Accuracy of partial, charge models and optimization of nonpolar contributions. *J. Chem. Theory. Comput.* **2006**, *2*, 128−139.
(11) Sitkoff, D.; Sharp, K. A.; Honig, B. Accurate Calculation of Hydration Free-Energies Using Macroscopic Solvent Models. *J. Phys. Chem.* **1994**, *98*, 1978−1988.
(12) Still, W. C.; Tempczyk, A.; Hawley, R. C.; Hendrickson, T. Semianalytical Treatment of Solvation for Molecular Mechanics and Dynamics. *J. Am. Chem. Soc.* **1990**, *112*, 6127−6129.
(13) Ferrari, A. M.; Degliesposti, G.; Sgobba, M.; Rastelli, G. Validation of an automated procedure for the prediction of relative free energies of binding on a set of aldose reductase inhibitors. *Bioorg. Med. Chem.* **2007**, *15*, 7865−7877.
(14) Kuhn, B.; Kollman, P. A. Binding of a diverse set of ligands to avidin and streptavidin: An accurate quantitative prediction of their relative affinities by a combination of molecular mechanics and continuum solvent models. *J. Med. Chem.* **2000**, *43*, 3786−3791.
(15) Rastelli, G.; Del Rio, A.; Degliesposti, G.; Sgobba, M. Fast and accurate predictions of binding free energies using MM-PBSA and MM-GBSA. *J. Comput. Chem.* **2010**, *31*, 797−810.
(16) Wang, W.; Kollman, P. A. Free energy calculations on dimer stability of the HIV protease using molecular dynamics and a continuum solvent model. *J. Mol. Biol.* **2000**, *303*, 567−582.
(17) Brice, A. R.; Dominy, B. N. Analyzing the robustness of the MM/PBSA free energy calculation method: application to DNA conformational transitions. *J. Comput. Chem.* **2011**, *32*, 1431−1440.
(18) Brown, S. P.; Muchmore, S. W. Large-scale application of high-throughput molecular mechanics with Poisson-Boltzmann surface area for routine physics-based scoring of protein-ligand complexes. *J. Med. Chem.* **2009**, *52*, 3159−3165.
(19) Weis, A.; Katebzadeh, K.; Soderhjelm, P.; Nilsson, I.; Ryde, U. Ligand affinities predicted with the MM/PBSA method: dependence on the simulation method and the force field. *J. Med. Chem.* **2006**, *49*, 6596−6606.
(20) Kumar, R.; Shinde, R. N.; Ajay, D.; Sobhia, M. E. Probing interaction requirements in PTP1B inhibitors: a comparative molecular dynamics study. *J. Chem. Inf. Model.* **2010**, *50*, 1147−1158.
(21) Wang, W.; Kollman, P. A. Computational study of protein specificity: the molecular basis of HIV-1 protease drug resistance. *Proc. Natl. Acad. Sci. USA* **2001**, *98*, 14937−14942.
(22) Venken, T.; Krnavek, D.; Munch, J.; Kirchhoff, F.; Henklein, P.; De Maeyer, M.; Voet, A. An optimized MM/PBSA virtual screening approach applied to an HIV-1 gp41 fusion peptide inhibitor. *Proteins* **2011**, *79*, 3221−3235.
(23) Meliciani, I.; Klenin, K.; Strunk, T.; Schmitz, K.; Wenzel, W. Probing hot spots on protein-protein interfaces with all-atom free-energy simulation. *J. Chem. Phys.* **2009**, *131*, 034114.
(24) Zoete, V.; Meuwly, M.; Karplus, M. Study of the insulin dimerization: binding free energy calculations and per-residue free energy decomposition. *Proteins* **2005**, *61*, 79−93.
(25) Degliesposti, G.; Portioli, C.; Parenti, M. D.; Rastelli, G. BEAR, a novel virtual screening methodology for drug discovery. *J. Biomol. Screen.* **2011**, *16*, 129−133.
(26) Lindström, A.; Edvinsson, L.; Johansson, A.; Andersson, C. D.; Andersson, I. E.; Raubacher, F.; Linusson, A. Postprocessing of Docked Protein−Ligand Complexes Using Implicit Solvation Models. *J. Chem. Inf. Model.* **2011**, *51*, 267−282.
(27) Rastelli, G.; Degliesposti, G.; Del Rio, A.; Sgobba, M. Binding estimation after refinement, a new automated procedure for the refinement and rescoring of docked ligands in virtual screening. *Chem. Biol. Drug. Des.* **2009**, *73*, 283−286.
(28) Barakat, K. H.; Jordheim, L. P.; Perez-Pineiro, R.; Wishart, D.; Dumontet, C.; Tuszynski, J. A. Virtual screening and biological evaluation of inhibitors targeting the XPA-ERCC1 interaction. *PLoS One* **2012**, *7*, e51329.
(29) Yang, T.; Wu, J. C.; Yan, C.; Wang, Y.; Luo, R.; Gonzales, M. B.; Dalby, K. N.; Ren, P. Virtual screening using molecular simulations. *Proteins* **2011**, *79*, 1940−1951.
(30) Kasam, V.; Salzemann, J.; Botha, M.; Dacosta, A.; Degliesposti, G.; Isea, R.; Kim, D.; Maass, A.; Kenyon, C.; Rastelli, G.; Hofmann-Apitius, M.; Breton, V. WISDOM-II: Screening against multiple targets implicated in malaria using computational grid infrastructures. *Malar. J.* **2009**, *8*, 88.
(31) Case, D. A.; Cheatham, T. E.; Darden, T.; Gohlke, H.; Luo, R.; Merz, K. M.; Onufriev, A.; Simmerling, C.; Wang, B.; Woods, R. J. The Amber biomolecular simulation programs. *J. Comput. Chem.* **2005**, *26*, 1668−1688.
(32) Pronk, S.; Pall, S.; Schulz, R.; Larsson, P.; Bjelkmar, P.; Apostolov, R.; Shirts, M. R.; Smith, J. C.; Kasson, P. M.; van der Spoel, D.; Hess, B.; Lindahl, E. GROMACS 4.5: a high-throughput and highly parallel open source molecular simulation toolkit. *Bioinformatics* **2013**, *29*, 845−854.

(33) Li, L.; Li, C.; Sarkar, S.; Zhang, J.; Witham, S.; Zhang, Z.; Wang, L.; Smith, N.; Petukh, M.; Alexov, E. DelPhi: a comprehensive suite for DelPhi software and associated resources. *BMC Biophys* **2012**, *5*, 9.
(34) Baker, N. A.; Sept, D.; Joseph, S.; Holst, M. J.; McCammon, J. A. Electrostatics of nanosystems: application to microtubules and the ribosome. *Proc. Natl. Acad. Sci. USA* **2001**, *98*, 10037−10041.
(35) Chiang, H. L.; Ngo, S. T.; Chen, C. J.; Hu, C. K.; Li, M. S. Oligomerization of Peptides LVEALYL and RGFFYT and Their Binding Affinity to Insulin. *PLoS One* **2013**, *8*, e65358.
(36) Ganoth, A.; Friedman, R.; Nachliel, E.; Gutman, M. A molecular dynamics study and free energy analysis of complexes between the Mlc1p protein and two IQ motif peptides. *Biophys. J.* **2006**, *91*, 2436−50.
(37) Spiliotopoulos, D.; Spitaleri, A.; Musco, G. Exploring PHD fingers and H3K4me0 interactions with molecular dynamics simulations and binding free energy calculations: AIRE-PHD1, a comparative study. *PLoS One* **2012**, *7*, e46902.
(38) Levy, R. M.; Zhang, L. Y.; Gallicchio, E.; Felts, A. K. On the nonpolar hydration free energy of proteins: surface area and continuum solvent models for the solute-solvent interaction energy. *J. Am. Chem. Soc.* **2003**, *125*, 9523−9530.
(39) Tan, C.; Tan, Y. H.; Luo, R. Implicit nonpolar solvent models. *J. Phys. Chem. B* **2007**, *111*, 12263−12274.
(40) Wagoner, J. A.; Baker, N. A. Assessing implicit models for nonpolar mean solvation forces: the importance of dispersion and volume terms. *Proc. Natl. Acad. Sci. USA* **2006**, *103*, 8331−8336.
(41) Phillips, J. C.; Braun, R.; Wang, W.; Gumbart, J.; Tajkhorshid, E.; Villa, E.; Chipot, C.; Skeel, R. D.; Kale, L.; Schulten, K. Scalable molecular dynamics with NAMD. *J. Comput. Chem.* **2005**, *26*, 1781−802.
(42) Pearlman, D. A.; Charifson, P. S. Are free energy calculations useful in practice? A comparison with rapid scoring functions for the p38 MAP kinase protein system. *J. Med. Chem.* **2001**, *44*, 3417−23.
(43) Hou, T.; McLaughlin, W. A.; Wang, W. Evaluating the potency of HIV-1 protease drugs to combat resistance. *Proteins* **2008**, *71*, 1163−1174.
(44) Hou, T.; Yu, R. Molecular dynamics and free energy studies on the wild-type and double mutant HIV-1 protease complexed with amprenavir and two amprenavir-related inhibitors: mechanism for binding and drug resistance. *J. Med. Chem.* **2007**, *50*, 1177−1188.
(45) Kar, P.; Knecht, V. Origin of decrease in potency of darunavir and two related antiviral inhibitors against HIV-2 compared to HIV-1 protease. *J. Phys. Chem. B* **2012**, *116*, 2605−2614.
(46) Srinivasan, J.; Cheatham, T. E.; Cieplak, P.; Kollman, P. A.; Case, D. A. Continuum solvent studies of the stability of DNA, RNA, and phosphoramidate - DNA helices. *J. Am. Chem. Soc.* **1998**, *120*, 9401−9409.
(47) Lee, M. R.; Duan, Y.; Kollman, P. A. Use of MM-PB/SA in estimating the free energies of proteins: Application to native, intermediates, and unfolded villin headpiece. *Proteins* **2000**, *39*, 309−316.
(48) Hornak, V.; Abel, R.; Okur, A.; Strockbine, B.; Roitberg, A.; Simmerling, C. Comparison of multiple Amber force fields and development of improved protein backbone parameters. *Proteins* **2006**, *65*, 712−725.
(49) Lindorff-Larsen, K.; Piana, S.; Palmo, K.; Maragakis, P.; Klepeis, J. L.; Dror, R. O.; Shaw, D. E. Improved side-chain torsion potentials for the Amber ff99SB protein force field. *Proteins* **2010**, *78*, 1950−1958.
(50) Wang, J.; Wolf, R. M.; Caldwell, J. W.; Kollman, P. A.; Case, D. A. Development and testing of a general amber force field. *J. Comput. Chem.* **2004**, *25*, 1157−1174.
(51) Honig, B.; Nicholls, A. Classical Electrostatics in Biology and Chemistry. *Science* **1995**, *268*, 1144−1149.
(52) Hunenberger, P. H.; Helms, V.; Narayana, N.; Taylor, S. S.; McCammon, J. A. Determinants of ligand binding to cAMP-dependent protein kinase. *Biochemistry* **1999**, *38*, 2358−2366.
(53) Dzubiella, J.; Swanson, J. M. J.; McCammon, J. A. Coupling nonpolar and polar solvation free energies in implicit solvent models. *J. Chem. Phys.* **2006**, *124*, 084905.
(54) Hummer, G. Hydrophobic force field as a molecular alternative to surface-area models. *J. Am. Chem. Soc.* **1999**, *121*, 6299−6305.
(55) Kang, Y. K.; Nemethy, G.; Scheraga, H. A. Free-Energies of Hydration of Solute Molecules 0.1. Improvement of the Hydration Shell-Model by Exact Computations of Overlapping Volumes. *J. Phys. Chem.* **1987**, *91*, 4105−4109.
(56) Smith, R.; Tanford, C. Hydrophobicity of Long-Chain Alkyl Carboxylic-Acids, as Measured by Their Distribution between Heptane and Aqueous-Solutions. *Proc. Natl. Acad. Sci. USA* **1973**, *70*, 289−293.
(57) Lum, K.; Chandler, D.; Weeks, J. D. Hydrophobicity at small and large length scales. *J. Phys. Chem. B* **1999**, *103*, 4570−4577.
(58) Pierotti, R. A. Scaled Particle Theory of Aqueous and Non-Aqueous Solutions. *Chem. Rev.* **1976**, *76*, 717−726.
(59) Weeks, J. D.; Chandler, D.; Andersen, H. C. Role of Repulsive Forces in Determining Equilibrium Structure of Simple Liquids. *J. Chem. Phys.* **1971**, *54*, 5237−5247.
(60) Konecny, R.; Baker, N. A.; McCammon, J. A. iAPBS: a programming interface to Adaptive Poisson-Boltzmann Solver (APBS). *Comput. Sci. Discov.* **2012**, 5.
(61) Brooks, B. R.; Brooks, C. L., 3rd; Mackerell, A. D., Jr.; Nilsson, L.; Petrella, R. J.; Roux, B.; Won, Y.; Archontis, G.; Bartels, C.; Boresch, S.; Caflisch, A.; Caves, L.; Cui, Q.; Dinner, A. R.; Feig, M.; Fischer, S.; Gao, J.; Hodoscek, M.; Im, W.; Kuczera, K.; Lazaridis, T.; Ma, J.; Ovchinnikov, V.; Paci, E.; Pastor, R. W.; Post, C. B.; Pu, J. Z.; Schaefer, M.; Tidor, B.; Venable, R. M.; Woodcock, H. L.; Wu, X.; Yang, W.; York, D. M.; Karplus, M. CHARMM: the biomolecular simulation program. *J. Comput. Chem.* **2009**, *30*, 1545−614.
(62) Case, D. A.; Darden, T.; Cheatham, T. E., III; Simmerling, C. L.; Wang, J.; Duke, R. E.; Luo, R.; Walker, R. C.; Zhang, W.; Merz, K. M.; Roberts, B.; Hayik, S.; Roitberg, A.; Seabra, G.; Swails, J.; Goetz, A. W.; Kolossváry, I.; Wong, K. F.; Paesani, F.; Vanicek, J.; Wolf, R. M.; Liu, J.; Wu, X.; Brozell, S. R.; Steinbrecher, T.; Gohlke, H.; Cai, Q.; Ye, X.; Wang, J.; Hsieh, M.-J.; Cui, G.; Roe, D. R.; Mathews, D. H.; Seetin, M. G.; Salomon-Ferrer, R.; Sagui, C.; Babin, V.; Luchko, T.; Gusarov, S.; Kovalenko, A.; Kollman, P. A. *AMBER 12*, University of California: San Francisco, 2012.
(63) Tsui, V.; Case, D. A. Theory and applications of the generalized Born solvation model in macromolecular Simulations. *Biopolymers* **2001**, *56*, 275−291.
(64) Tsui, V.; Case, D. A. Molecular dynamics simulations of nucleic acids with a generalized born solvation model. *J. Am. Chem. Soc.* **2000**, *122*, 2489−2498.
(65) Bondi, A. van der Waals Volumes and Radii. *J. Phys. Chem.* **1964**, *68*, 441−451.
(66) Eisenhaber, F.; Lijnzaad, P.; Argos, P.; Sander, C.; Scharf, M. The Double Cubic Lattice Method - Efficient Approaches to Numerical-Integration of Surface-Area and Volume and to Dot Surface Contouring of Molecular Assemblies. *J. Comput. Chem.* **1995**, *16*, 273−284.
(67) O'Boyle, N. M.; Banck, M.; James, C. A.; Morley, C.; Vandermeersch, T.; Hutchison, G. R. Open Babel: An open chemical toolbox. *J. Cheminform.* **2011**, *3*, 33.
(68) Jakalian, A.; Jack, D. B.; Bayly, C. I. Fast, efficient generation of high-quality atomic charges. AM1-BCC model: II. Parameterization and validation. *J. Comput. Chem.* **2002**, *23*, 1623−1641.
(69) Wang, J.; Wang, W.; Kollman, P. A.; Case, D. A. Automatic atom type and bond type perception in molecular mechanical calculations. *J. Mol. Graph. Model.* **2006**, *25*, 247−260.
(70) Sousa da Silva, A. W.; Vranken, W. F. ACPYPE - AnteChamber PYthon Parser interfacE. *BMC Res. Notes* **2012**, *5*, 367.
(71) Sondergaard, C. R.; Olsson, M. H. M.; Rostkowski, M.; Jensen, J. H. Improved Treatment of Ligands and Coupling Effects in Empirical Calculation and Rationalization of pK(a) Values. *J. Chem. Theory. Comput.* **2011**, *7*, 2284−2295.

(72) Jorgensen, W. L.; Chandrasekhar, J.; Madura, J. D.; Impey, R. W.; Klein, M. L. Comparison of Simple Potential Functions for Simulating Liquid Water. *J. Chem. Phys.* **1983**, *79*, 926−935.
(73) Berendsen, H. J. C.; Postma, J. P. M.; Vangunsteren, W. F.; Dinola, A.; Haak, J. R. Molecular-Dynamics with Coupling to an External Bath. *J. Chem. Phys.* **1984**, *81*, 3684−3690.
(74) Bussi, G.; Donadio, D.; Parrinello, M. Canonical sampling through velocity rescaling. *J. Chem. Phys.* **2007**, *126*, 014101.
(75) Nose, S.; Klein, M. L. Constant Pressure Molecular-Dynamics for Molecular-Systems. *Mol. Phys.* **1983**, *50*, 1055−1076.
(76) Darden, T.; York, D.; Pedersen, L. Particle Mesh Ewald - an N.Log(N) Method for Ewald Sums in Large Systems. *J. Chem. Phys.* **1993**, *98*, 10089−10092.
(77) Hess, B. P-LINCS: A parallel linear constraint solver for molecular simulation. *J. Chem. Theory. Comput.* **2008**, *4*, 116−122.
(78) Hess, B.; Bekker, H.; Berendsen, H. J. C.; Fraaije, J. G. E. M. LINCS: A linear constraint solver for molecular simulations. *J. Comput. Chem.* **1997**, *18*, 1463−1472.
(79) Cheng, Y.; Prusoff, W. H. Relationship between the inhibition constant (K1) and the concentration of inhibitor which causes 50% inhibition (I50) of an enzymatic reaction. *Biochem. Pharmacol.* **1973**, *22*, 3099−108.
(80) Hou, T.; Wang, J.; Li, Y.; Wang, W. Assessing the performance of the molecular mechanics/Poisson Boltzmann surface area and molecular mechanics/generalized Born surface area methods. II. The accuracy of ranking poses generated from docking. *J. Comput. Chem.* **2011**, *32*, 866−877.
(81) Hou, T.; Wang, J.; Li, Y.; Wang, W. Assessing the performance of the MM/PBSA and MM/GBSA methods. 1. The accuracy of binding free energy calculations based on molecular dynamics simulations. *J. Chem. Inf. Model.* **2011**, *51*, 69−82.
(82) Levitt, M.; Sander, C.; Stern, P. S. Protein Normal-Mode Dynamics - Trypsin-Inhibitor, Crambin, Ribonuclease and Lysozyme. *J. Mol. Biol.* **1985**, *181*, 423−447.
(83) Hagler, A. T.; Stern, P. S.; Sharon, R.; Becker, J. M.; Naider, F. Computer-Simulation of the Conformational Properties of Oligopeptides - Comparison of Theoretical Methods and Analysis of Experimental Results. *J. Am. Chem. Soc.* **1979**, *101*, 6842−6852.
(84) Kopitz, H.; Cashman, D. A.; Pfeiffer-Marek, S.; Gohlke, H. Influence of the Solvent Representation on Vibrational Entropy Calculations: Generalized Born Versus Distance-Dependent Dielectric Model. *J. Comput. Chem.* **2012**, *33*, 1004−1013.
(85) Hensen, U.; Lange, O. F.; Grubmuller, H. Estimating Absolute Configurational Entropies of Macromolecules: The Minimally Coupled Subspace Approach. *PLoS One* **2010**, *5*, e9179.
(86) Chang, C. E. A.; Chen, W.; Gilson, M. K. Ligand configurational entropy and protein binding. *Proc. Natl. Acad. Sci. USA* **2007**, *104*, 1534−1539.
(87) Andricioaei, I.; Karplus, M. On the calculation of entropy from covariance matrices of the atomic fluctuations. *J. Chem. Phys.* **2001**, *115*, 6289−6292.
(88) Tidor, B.; Karplus, M. The Contribution of Vibrational Entropy to Molecular Association - the Dimerization of Insulin. *J. Mol. Biol.* **1994**, *238*, 405−414.
(89) Schlitter, J. Estimation of Absolute and Relative Entropies of Macromolecules Using the Covariance-Matrix. *Chem. Phys. Lett.* **1993**, *215*, 617−621.
(90) Srivastava, H. K.; Sastry, G. N. Molecular dynamics investigation on a series of HIV protease inhibitors: assessing the performance of MM-PBSA and MM-GBSA approaches. *J. Chem. Inf. Model.* **2012**, *52*, 3088−3098.
(91) Kongsted, J.; Soderhjelm, P.; Ryde, U. How accurate are continuum solvation models for drug-like molecules? *J. Comput. Aided. Mol. Des.* **2009**, *23*, 395−409.
(92) Tan, C.; Yang, L.; Luo, R. How well does Poisson-Boltzmann implicit solvent agree with explicit solvent? A quantitative analysis. *J. Phys. Chem. B* **2006**, *110*, 18680−18687.
(93) Harris, R. C.; Boschitsch, A. H.; Fenley, M. O. Influence of Grid Spacing in Poisson-Boltzmann Equation Binding Energy Estimation. *J. Chem. Theory. Comput.* **2013**, *9*, 3677−3685.
(94) Simonson, T.; Brooks, C. L. Charge screening and the dielectric constant of proteins: Insights from molecular dynamics. *J. Am. Chem. Soc.* **1996**, *118*, 8452−8458.
(95) Wang, J.; Cai, Q.; Xiang, Y.; Luo, R. Reducing grid-dependence in finite-difference Poisson-Boltzmann calculations. *J. Chem. Theory. Comput.* **2012**, *8*, 2741−2751.
(96) Rocchia, W.; Sridharan, S.; Nicholls, A.; Alexov, E.; Chiabrera, A.; Honig, B. Rapid grid-based construction of the molecular surface and the use of induced surface charge to calculate reaction field energies: Applications to the molecular systems and geometric objects. *J. Comput. Chem.* **2002**, *23*, 128−137.
(97) Gilson, M. K.; Sharp, K. A.; Honig, B. H. Calculating the electrostatic potential of molecules in solution: Method and error assessment. *J. Comput. Chem.* **1988**, *9*, 327−335.
(98) Bruccoleri, R. E.; Novotny, J.; Davis, M. E.; Sharp, K. A. Finite difference Poisson-Boltzmann electrostatic calculations: Increased accuracy achieved by harmonic dielectric smoothing and charge antialiasing. *J. Comput. Chem.* **1997**, *18*, 268−276.
(99) Im, W.; Beglov, D.; Roux, B. Continuum solvation model: Computation of electrostatic forces from numerical solutions to the Poisson-Boltzmann equation. *Comput. Phys. Commun.* **1998**, *111*, 59−75.
(100) Nina, M.; Im, W.; Roux, B. Optimized atomic radii for protein continuum electrostatics solvation forces. *Biophys. Chem.* **1999**, *78*, 89−96.
(101) Oehme, D. P.; Brownlee, R. T.; Wilson, D. J. Effect of atomic charge, solvation, entropy, and ligand protonation state on MM-PB(GB)SA binding energies of HIV protease. *J. Comput. Chem.* **2012**, *33*, 2566−2580.
(102) Thompson, D. C.; Humblet, C.; Joseph-McCarthy, D. Investigation of MM-PBSA rescoring of docking poses. *J. Chem. Inf. Model.* **2008**, *48*, 1081−1091.